NATIONAL ADVISORY COMMITTEE FOR AERONAUTICS

TECHNICAL NOTE 1924

ESTIMATION OF THE DAMPING IN ROLL OF WINGS THROUGH THE NORMAL FLIGHT RANGE OF LIFT COEFFICIENT

By Alex Goodman and Glenn H. Adair

Langley Aeronautical Laboratory
Langley Air Force Base, Va.

Washington
July 1949

NATIONAL ADVISORY COMMITTEE FOR AERONAUTICS

TECHNICAL NOTE 1924

ESTIMATION OF THE DAMPING IN ROLL OF WINGS THROUGH THE NORMAL FLIGHT RANGE OF LIFT COEFFICIENT

By Alex Goodman and Glenn H. Adair

SUMMARY

Three methods have been developed for estimating the damping in roll through the normal flight range of lift coefficient for wing plan forms having various sweep angles, aspect ratios, and taper ratios.

Values of the damping in roll calculated by the three methods were compared with experimental values. The most complete method in which all known factors affecting the damping in roll were considered appeared to give the best quantitative agreement with experiment for approximately 60 percent of the cases investigated. Another method, in which the value of the damping in roll at zero lift coefficient is modified only in accordance with variations in finite-span lift-curve slope, is almost as reliable as the most complete method. The most important factor considered in the analysis therefore appears to be the variation of the finite-span lift-curve slope.

INTRODUCTION

Results of tests conducted on swept wings (reference 1, for example) have indicated that, although the present theories used to calculate the damping in roll (references 2 to 6) are quite accurate at the low lift coefficients, large discrepancies may exist at moderate and high lift coefficients.

The present analysis was made to determine the factors that contribute to the discrepancies at high lift coefficients and to devise procedures by which improved estimates could be made. The procedures developed from the present analysis are based on simplified theoretical concepts and utilize measured lift and drag data.

Comparisons are presented between experimental values of the damping in roll and values estimated by three methods.

SYMBOLS

The symbols used in the analysis and in the presentation of the results are defined herein.

C_L	lift coefficient	$\left(\frac{\text{Lift}}{\frac{1}{2}\rho V^2 S}\right)$
C_D	drag coefficient	$\left(\frac{\text{Drag}}{\frac{1}{2}\rho V^2 S}\right)$
C_l	rolling-moment coefficient	$\left(\frac{\text{Rolling moment}}{\frac{1}{2}\rho V^2 S b}\right)$
C_n	yawing-moment coefficient	$\left(\frac{\text{Yawing moment}}{\frac{1}{2}\rho V^2 S b}\right)$
ρ	mass density of air	
S	wing area	
V	flight velocity	
b	wing span, measured perpendicular to plane of symmetry	
y	spanwise distance from plane of symmetry to any section on wing quarter-chord line	
α	angle of attack, measured in plane of symmetry	
Λ	sweep angle of wing quarter-chord line, positive for sweepback	
A	aspect ratio $\left(b^2/S\right)$	

λ taper ratio $\left(\frac{\text{Tip chord}}{\text{Root chord}}\right)$

$pb/2V$ wing-tip helix angle

p angular velocity about X-axis

a_o section lift-curve slope

c_2 section primary force coefficient (see reference 4)

$C_{L_\alpha} = \frac{\partial C_L}{\partial \alpha}$

$C_{l_p} = \frac{\partial C_l}{\partial \left(\frac{pb}{2V}\right)}$

$C_{n_p} = \frac{\partial C_n}{\partial \left(\frac{pb}{2V}\right)}$

K_1, K_2 constants that are functions of wing plan form

$\beta = \sqrt{1 - M^2 \cos^2 \Lambda}$

M Mach number $\left(\frac{\text{Velocity of free stream}}{\text{Velocity of sound}}\right)$

Subscripts:

i induced

o profile

C_L at any lift coefficient unless specified differently

R right wing panel

L left wing panel

M at any Mach number unless specified differently

ANALYSIS

Development of Methods

The fact that the damping in roll is a function of both the lift-curve slope and the drag has been demonstrated by Glauert (reference 7). In most instances, for straight wings of moderately high aspect ratio, the lift-curve slope changes little through the lift-coefficient range and the drag contribution is relatively unimportant. Potential-flow values of C_{l_p} at zero lift coefficient, therefore, have generally been considered satisfactory at all lift coefficients below the stall.

A brief summary of the methods for calculating C_{l_p} at zero lift presented in references 2 to 6 is given herein.

Charts presenting values of the damping in roll based on lifting-line theory at zero lift coefficient for unswept wings having various aspect ratios and taper ratios are given in reference 2. These values were calculated from spanwise lift distributions that correspond to the rolling motion. The results given in reference 2 were corrected for lifting-surface effects by application of an effective edge-velocity correction in reference 3. An approximate method of modifying the results of reference 3 for the effects of sweep is presented in reference 4. A similar, but more refined, method which accounts for the effects of sweep on the edge-velocity correction factor is given in reference 5. A more rigorous method of calculating C_{l_p} for wings of arbitrary plan form at zero lift coefficient is presented in reference 6. This method consists of an application of the theory of Weissinger (reference 8) for determining the additional span loading during roll.

The values for the damping in roll presented in reference 6 are considered to be the most reliable and are used herein at zero lift coefficient. The results from reference 6 have been extended to an aspect ratio of 10 and are presented in figure 1. The values of $\left(C_{l_p}\right)_{C_L=0}$ presented in figure 1 are for a section lift-curve slope of 2π. The methods of reference 4 provide a convenient basis for correcting these results to any value of section lift-curve slope. As

indicated in reference 6, the correction is

$$\frac{\left(C_{l_p}\right)_{a_o}}{\left(C_{l_p}\right)_{2\pi}} = \frac{A + 4 \cos \Lambda}{\left(\frac{2\pi}{a_o}\right) A + 4 \cos \Lambda} \tag{1}$$

For low-aspect-ratio or swept wings of the type considered for high-speed flight, the finite-span lift-curve slope may vary considerably through the lift-coefficient range and the drag at high lift coefficients may become large. A procedure based on potential-flow considerations for calculating C_{l_p} at high lift coefficients can hardly be expected, therefore, since such behavior is associated with separation of flow that results in important local changes in the characteristics.

The method of reference 4 can be used to demonstrate that, to a first approximation, variations in the lift-curve slope will affect C_{l_p} in the same proportion as C_{L_α}. Therefore, if the effects of drag are neglected, C_{l_p} can be written as

$$C_{l_p} = \left(C_{l_p}\right)_{C_L=0} \frac{\left(C_{L_\alpha}\right)_{C_L}}{\left(C_{L_\alpha}\right)_{C_L=0}} \tag{2}$$

An analysis of the drag contribution for straight wings of elliptic-chord distribution (reference 9) indicates that the increment of C_{l_p} due to drag is equal to $\frac{1}{8} C_D$. If the same increment can be applied to swept wings, the resulting expression for C_{l_p} is

$$C_{l_p} = \left(C_{l_p}\right)_{C_L=0} \frac{\left(C_{L_\alpha}\right)_{C_L}}{\left(C_{L_\alpha}\right)_{C_L=0}} - \frac{1}{8} C_D \tag{3}$$

The problem of accounting for the drag of swept wings is actually somewhat more complicated than indicated by equation (3) since the profile drag and induced drag are not of equal importance and, therefore, must be considered separately. That is,

$$C_{l_p} = \left(C_{l_p}\right)_{C_L=0} \frac{\left(C_{L_\alpha}\right)_{C_L}}{\left(C_{L_\alpha}\right)_{C_L=0}} - K_1 C_{D_i} - K_2 C_{D_o} \tag{4}$$

in which the assumption is made that

$$C_{D_o} = C_D - \frac{C_L^2}{\pi A}$$

and K_1 and K_2 are constants that are functions of the wing plan form.

According to the strip-theory procedure of reference 4, the induced-drag contribution to C_{l_p} can be derived as follows.

The rolling moment due to induced drag for a constant-chord swept wing in roll can be expressed as

$$C_l = \frac{1}{b^2} \int_0^{b/2} \left[c_{2_L} \sin \Lambda \tan \Lambda \left(\alpha - \frac{py}{V}\right) - c_{2_R} \sin \Lambda \tan \Lambda \left(\alpha + \frac{py}{V}\right) - c_{2_L} \cos \Lambda \frac{py}{V} - c_{2_R} \cos \Lambda \frac{py}{V} \right] y \, dy \tag{5}$$

where, as indicated in reference 4,

$$c_{2_L} = \frac{1}{\pi A \cos \Lambda}\left(C_L - \frac{Aa_o \cos \Lambda}{A + 4 \cos \Lambda} \frac{y}{b/2} \frac{pb}{2V}\right)^2$$

$$c_{2_R} = \frac{1}{\pi A \cos \Lambda}\left(C_L + \frac{Aa_o \cos \Lambda}{A + 4 \cos \Lambda} \frac{y}{b/2} \frac{pb}{2V}\right)^2$$

Substituting the values c_{2_L} and c_{2_R} in equation (5), performing the integration, differentiating with respect to $pb/2V$, and assuming $a_o = 2\pi$ result in the following expression:

$$\left(C_{l_p}\right)_{C_{D_i}} = -\frac{1}{6} \frac{C_L^2}{\pi A \cos^2 \Lambda}\left(1 + 2 \sin^2 \Lambda \frac{A + 2 \cos \Lambda}{A + 4 \cos \Lambda}\right) \qquad (6)$$

For zero sweep this expression reduces to

$$\left(C_{l_p}\right)_{C_{D_i}} = -\frac{1}{6} \frac{C_L^2}{\pi A}$$

which is in agreement with the result given in reference 9 for constant-chord wings. It can be demonstrated that for swept wings having elliptic-chord distributions, the constant $1/6$ in equation (6) is replaced by $1/8$, as was used in connection with the total-drag term in equation (3). The constant corresponding to the elliptic-chord distribution is regarded as being more reliable for wings of practical design, and therefore the induced-drag contribution to C_{l_p} can be

written as

$$\left(C_{l_p}\right)_{C_{D_i}} = -\frac{1}{8}\frac{C_L^2}{\pi A \cos^2 \Lambda}\left(1 + 2\sin^2\Lambda\,\frac{A + 2\cos\Lambda}{A + 4\cos\Lambda}\right) \tag{7}$$

Values obtained from equation (7) are presented in figure 2 as a plot of $\left(C_{l_p}\right)_{C_{D_i}} \Big/ C_L^2$ against aspect ratio for various sweep angles.

As in the case of the induced drag, the theoretical constant for the profile-drag contribution to C_{l_p} for an elliptic-chord distribution is 1/8, which is the same as for straight wings.

An equation for the damping in roll of swept wings, which accounts for the induced drag, the profile drag, and for variations in finite-span lift-curve slope, can therefore be written as

$$C_{l_p} = \left(C_{l_p}\right)_{C_L=0}\frac{\left(C_{L_\alpha}\right)_{C_L}}{\left(C_{L_\alpha}\right)_{C_L=0}} + \left(C_{l_p}\right)_{C_{D_i}} - \frac{1}{8}C_{D_o} \tag{8}$$

An attempt was made to evaluate empirical values of K_2 (equation (4)) by procedures similar to that used for C_{n_p} in reference 1, but the value of 1/8 appeared to be as good as any that could be obtained.

Application of Methods

From the foregoing analysis, three methods of calculating C_{l_p} are indicated by equations (2), (3), and (8):

Method 1

$$C_{l_p} = \left(C_{l_p}\right)_{C_L=0}\frac{\left(C_{L_\alpha}\right)_{C_L}}{\left(C_{L_\alpha}\right)_{C_L=0}}$$

Method 2

$$C_{l_p} = \left(C_{l_p}\right)_{C_L=0} \frac{\left(C_{L_\alpha}\right)_{C_L}}{\left(C_{L_\alpha}\right)_{C_L=0}} - \frac{1}{8} C_D$$

Method 3

$$C_{l_p} = \left(C_{l_p}\right)_{C_L=0} \frac{\left(C_{L_\alpha}\right)_{C_L}}{\left(C_{L_\alpha}\right)_{C_L=0}} + \left(C_{l_p}\right)_{C_{D_i}} - \frac{1}{8} C_{D_o}$$

The values of $\left(C_{l_p}\right)_{C_L=0}$ used in methods 1, 2, and 3 are presented in figure 1 for zero Mach number and a section lift-curve slope of 2π. As was previously pointed out, the values from figure 1 can be corrected to any section lift-curve slope by means of the relation

$$\frac{\left(C_{l_p}\right)_{a_o}}{\left(C_{l_p}\right)_{2\pi}} = \frac{A + 4 \cos \Lambda}{\left(\frac{2\pi}{a_o}\right) A + 4 \cos \Lambda}$$

Methods of applying corrections for the effects of compressibility, within the subcritical range of Mach number, are indicated in references 6 and 10. The method of reference 10, though less rigorous than that of reference 6, has been found to be about as reliable as and somewhat more convenient than the method of reference 6. According to reference 10, the correction for compressibility is

$$\left[\left(C_{l_p}\right)_{C_L=0}\right]_M = \frac{A + 4 \cos \Lambda}{A\beta + 4 \cos \Lambda} \left[\left(C_{l_p}\right)_{C_L=0}\right]_{M=0}$$

The ratio $\left(C_{L_\alpha}\right)_{C_L} \Big/ \left(C_{L_\alpha}\right)_{C_L=0}$ used in methods 1, 2, and 3 is defined as the ratio of the finite-span lift-curve slope at a particular lift coefficient to the finite-span lift-curve slope at zero lift coefficient. This ratio is obtained from the measured lift characteristics of the particular plan form. In order to estimate values of C_{l_p} at high Mach numbers the lift data corresponding to the particular Mach number should be used. Similarly, in method 2, the drag data corresponding to the particular Mach number should be used in order to account for compressibility effects.

The values of $\left(C_{l_p}\right)_{C_{D_i}}$ used in method 3 may be obtained from figure 2. Corrections to this increment for variations in section lift-curve slope or Mach number should not be necessary, since this increment is small except at high lift coefficients where the Mach number generally is low.

The profile-drag term C_{D_o} of method 3 is defined as

$$C_{D_o} = C_D - \frac{C_L^2}{\pi A}$$

where C_D and C_L should be taken from experimental data at the particular Mach number in question.

RESULTS AND DISCUSSION

Experimental data of C_{l_p} obtained for the wings listed in table I (taken from references 1, 11, and NACA tests) are compared in figures 3 to 17 with the results calculated by each of the three methods. The experimental data of C_L, C_D, and C_{D_o} used in the calculations are also presented.

Examination of figures 3 to 17 shows that method 1, in which the value of C_{l_p} at $C_L = 0$ is modified only in accordance with

variations in C_{L_α}, is almost as reliable as method 3. The variation of finite-span lift-curve slope therefore appears to be the most important factor considered in the analysis.

Method 3 shows a considerable error for the swept wings of aspect ratio 1.34 (wings 6 and 7) presented in figures 5 and 6. The error seems to result from the fact that the large values of $\left(C_{l_p}\right)_{C_{D_i}}$ indicated in figure 2 apparently are not realized for these wings. This result might be expected, since the assumptions regarding the distribution of forces on the wings could hardly be reliable at so low an aspect ratio.

Of these three methods, method 3, which includes separate considerations of the effects of induced and profile drag on C_{l_p}, appears to give the best quantitative agreement with experiment for approximately 60 percent of the cases investigated.

In the case of the two sweptforward wings presented in figure 15, the agreement between the experimental and calculated results is poor at the moderate and high lift coefficients. The large increase in C_{l_p} with lift coefficient for these wings is not accompanied by large changes in the variation of C_{L_α} with lift coefficient. This condition probably accounts for the poor agreement since, as has been pointed out, the variation in the finite-span lift-curve slope is the most important factor considered in the analysis.

CONCLUDING REMARKS

Three methods have been developed for estimating the damping in roll through the normal flight range of lift coefficient for wing plan forms having various sweep angles, aspect ratios, and taper ratios.

Values of the damping in roll calculated by the three methods were compared with experimental values. The most complete method (method 3) in which all known factors affecting the damping in roll were considered appeared to give the best quantitative agreement with experiment for approximately 60 percent of the cases investigated. Another method (method 1), in which the value of the damping in roll at zero lift coefficient is modified only in accordance with variations in finite-span lift-curve slope, is almost as reliable as the most

complete method. The most important factor considered in the analysis therefore appears to be the variation of the finite-span lift-curve slope.

Langley Aeronautical Laboratory
National Advisory Committee for Aeronautics
Langley Air Force Base, Va., June 7, 1949

REFERENCES

1. Goodman, Alex, and Fisher, Lewis R.: Investigation at Low Speeds of the Effect of Aspect Ratio and Sweep on Rolling Stability Derivatives of Untapered Wings. NACA TN 1835, 1949.

2. Pearson, Henry A., and Jones, Robert T.: Theoretical Stability and Control Characteristics of Wings with Various Amounts of Taper and Twist. NACA Rep. 635, 1938.

3. Swanson, Robert S., and Priddy, E. LaVerne: Lifting-Surface-Theory Values of the Damping in Roll and of the Parameter Used in Estimating Aileron Stick Forces. NACA ARR L5F23, 1945.

4. Toll, Thomas A., and Queijo, M. J.: Approximate Relations and Charts for Low-Speed Stability Derivatives of Swept Wings. NACA TN 1581, 1948.

5. Polhamus, Edward C.: A Simple Method of Estimating the Subsonic Lift and Damping in Roll of Sweptback Wings. NACA TN 1862, 1949.

6. Bird, John D.: Some Theoretical Low-Speed Span Loading Characteristics of Swept Wings in Roll and Sideslip. NACA TN 1839, 1949.

7. Glauert, H.: The Rotation of an Aerofoil about a Fixed Axis. R. & M. No. 595, British A.C.A., 1919.

8. Weissinger, J.: The Lift Distribution of Swept-Back Wings. NACA TM 1120, 1947.

9. Zimmerman, Charles H.: An Analysis of Lateral Stability in Power-Off Flight with Charts for Use in Design. NACA Rep. 589, 1937.

10. Fisher, Lewis R.: Approximate Corrections for the Effects of Compressibility on the Subsonic Stability Derivatives of Swept Wings. NACA TN 1854, 1949.

11. Bennett, Charles V., and Johnson, Joseph L.: Experimental Determination of the Damping in Roll and Aileron Rolling Effectiveness of Three Wings Having 2°, 42°, and 62° Sweepback. NACA TN 1278, 1947.

TABLE I

SUMMARY OF PERTINENT INFORMATION REGARDING WINGS CONSIDERED IN ANALYSIS

Wing	Sweep angle, Λ (deg)	Aspect ratio, A	Taper ratio, λ	Test Reynolds number	Airfoil section	Figure	Source
1	45	2.61	0.25	1.56×10^6	NACA 0012	3	NACA tests
2	45	2.61	.50	1.45	NACA 0012	3	
3	45	2.61	1.00	1.39	12 percent biconvex	4	
4	45	2.61	1.00	1.39	NACA 65_1-012	4	
5	0	1.34	1.00	1.99	NACA 0012	5	Reference 1
6	45	1.34	1.00	1.97	NACA 0012	5	
7	60	1.34	1.00	1.97	NACA 0012	6	
8	0	2.61	1.00	1.39	NACA 0012	6	
9	45	2.61	1.00	1.39	NACA 0012	7	
10	60	2.61	1.00	1.37	NACA 0012	7	
11	0	5.16	1.00	.98	NACA 0012	8	
12	45	5.16	1.00	.97	NACA 0012	8	
13	60	5.16	1.00	.76	NACA 0012	9	
14	2	10.00	.50	.163	Rhode St. Genese 33	9	Reference 11
15	42	5.90	.50	.231	Rhode St. Genese 33	10	
16	62	2.50	.50	.326	Rhode St. Genese 33	10	
17	0	4.62	.55	5.6	[a]NACA 0015	11	NACA tests
18	30	4.84	.44	6.20	[a]NACA 0015	11	
19	45	3.64	.42	7.80	[a]NACA 0015	12	
20	3.6	4.00	.60	.710	NACA 65A006	12	
21	32.6	4.00	.60	.710	NACA 65A006	13	
22	46.7	4.00	.60	.710	NACA 65A006	13	
23	36.9	4.00	0	1.23	NACA 0012	14	
24	52.2	2.31	0	1.62	NACA 0012	14	
25	-45	2.61	1.00	1.39	NACA 0012	15	
26	-45	3.12	.38	8.95	[a]NACA 0015	15	
27	45	4.00	.60	.710	NACA 65A008	16	
[b]28	45	4.00	.60	.710	NACA 65A008	16	
29	37.5	3.00	.49	1.02	NACA 23012	17	
[b]30	37.5	3.00	.49	1.02	NACA 23012	17	

[a]Varied from NACA 0015 section at root to NACA 23009 section at tip.
[b]Tested with full-span slats.

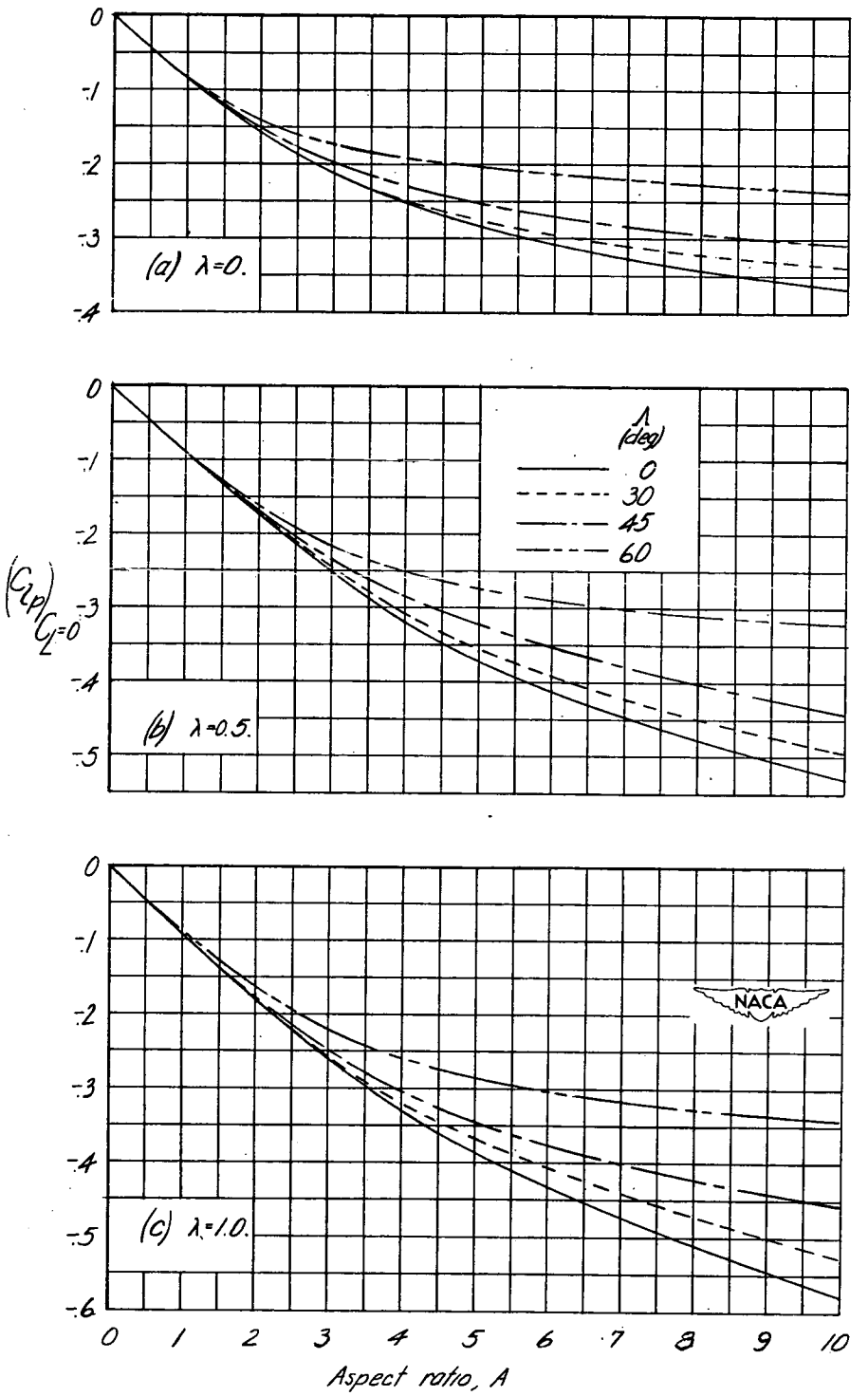

Figure 1.– Variation of $(C_{l_p})_{C_L=0}$ with aspect ratio for various sweep angles and taper ratios. $a_o = 2\pi$; M = 0.

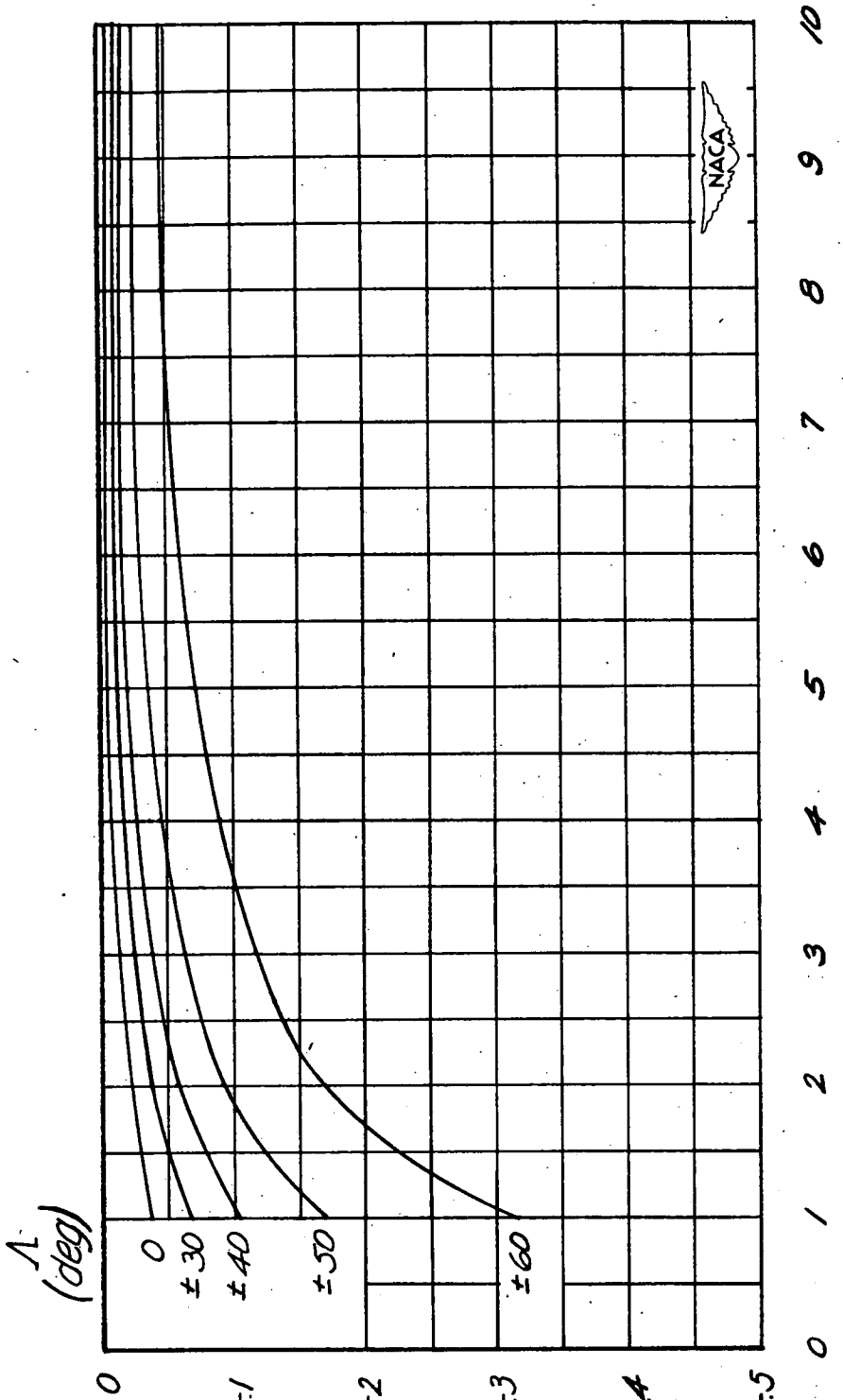

Figure 2.- Variation of $(C_{l_p})_{C_{D_i}}$ with aspect ratio for various sweep angles. $a_o = 2\pi$; M = 0.

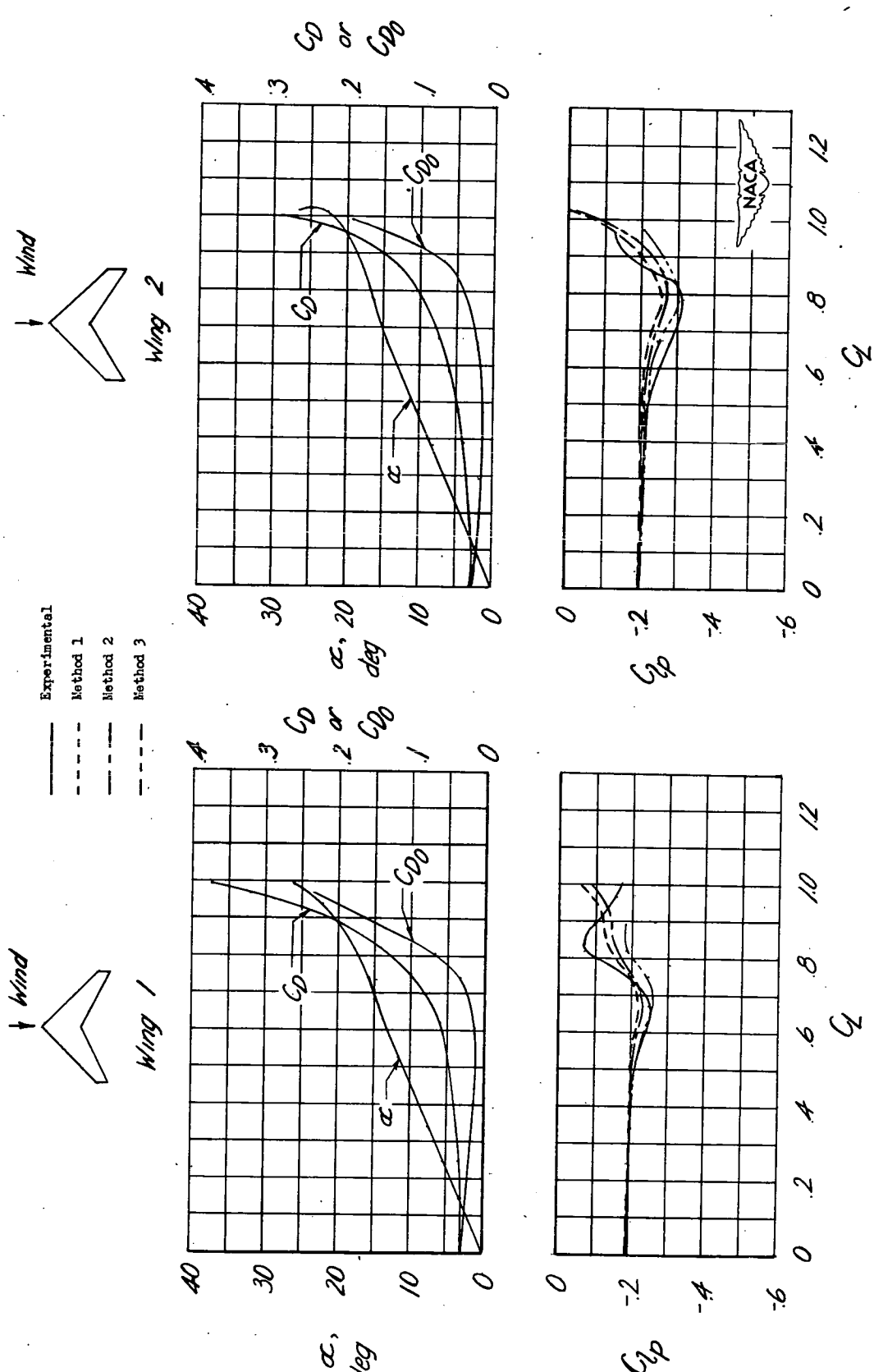

Figure 3.- Estimation of the damping in roll for wings 1 and 2.

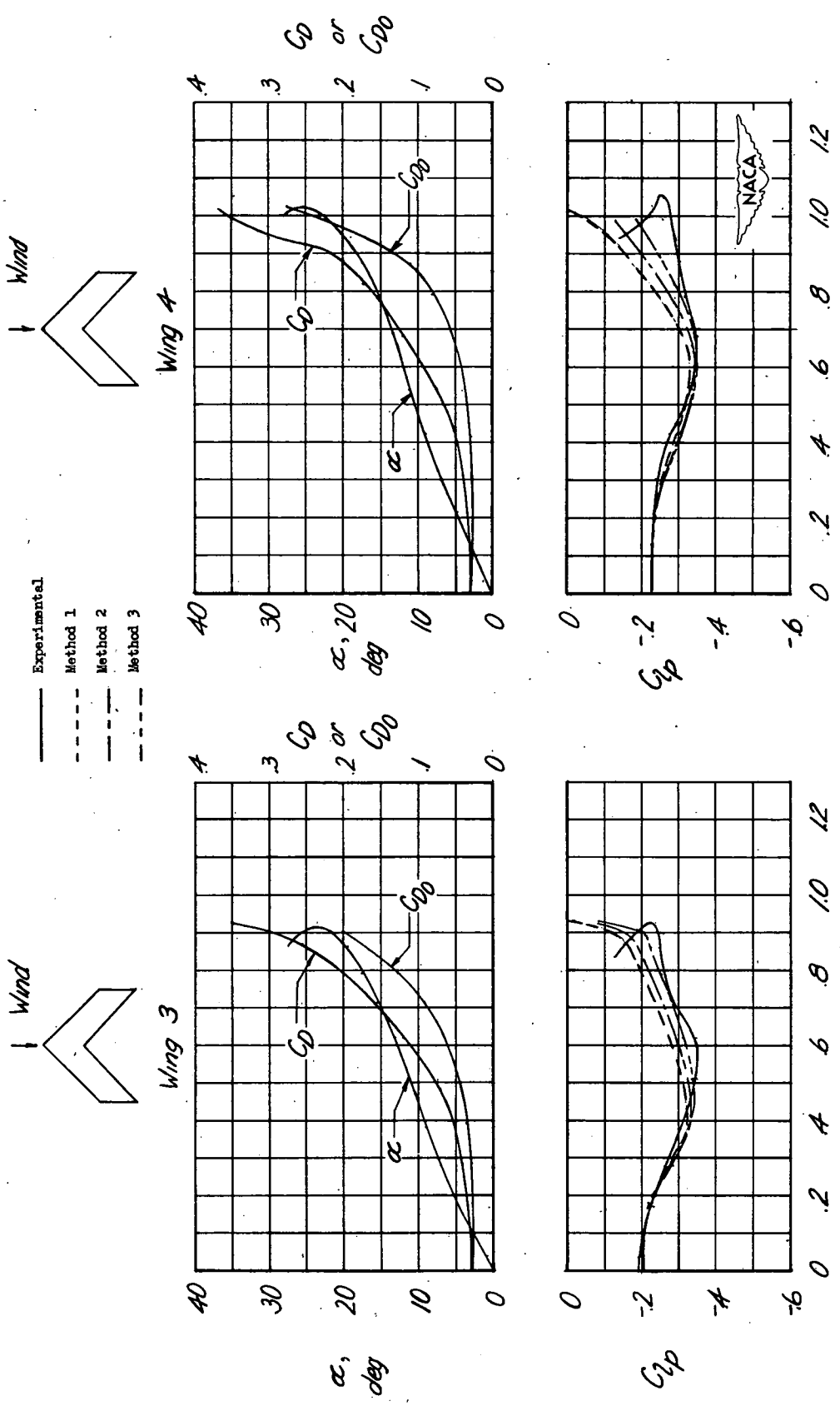

Figure 4.- Estimation of the damping in roll for wings 3 and 4.

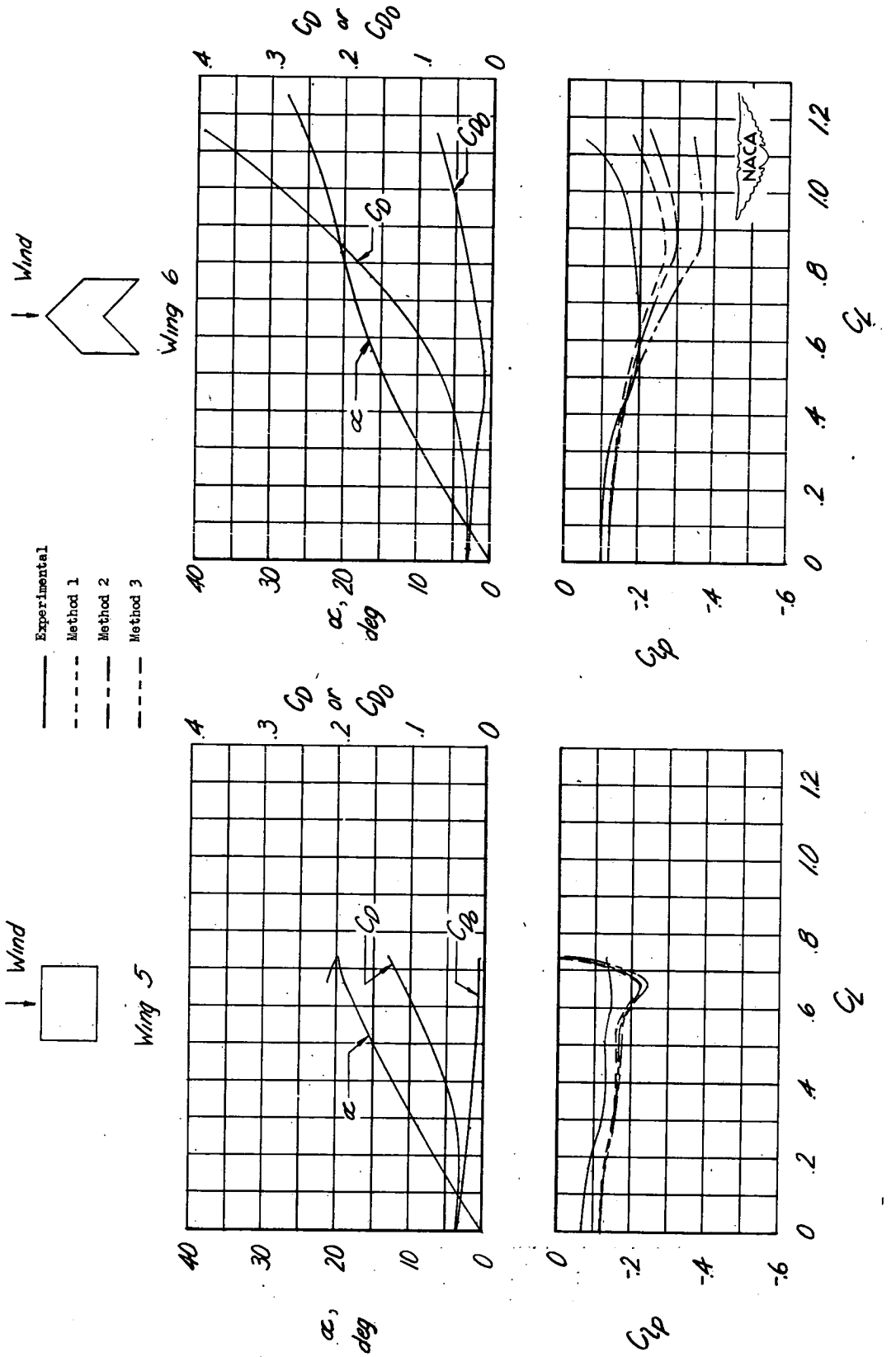

Figure 5.- Estimation of the damping in roll for wings 5 and 6.

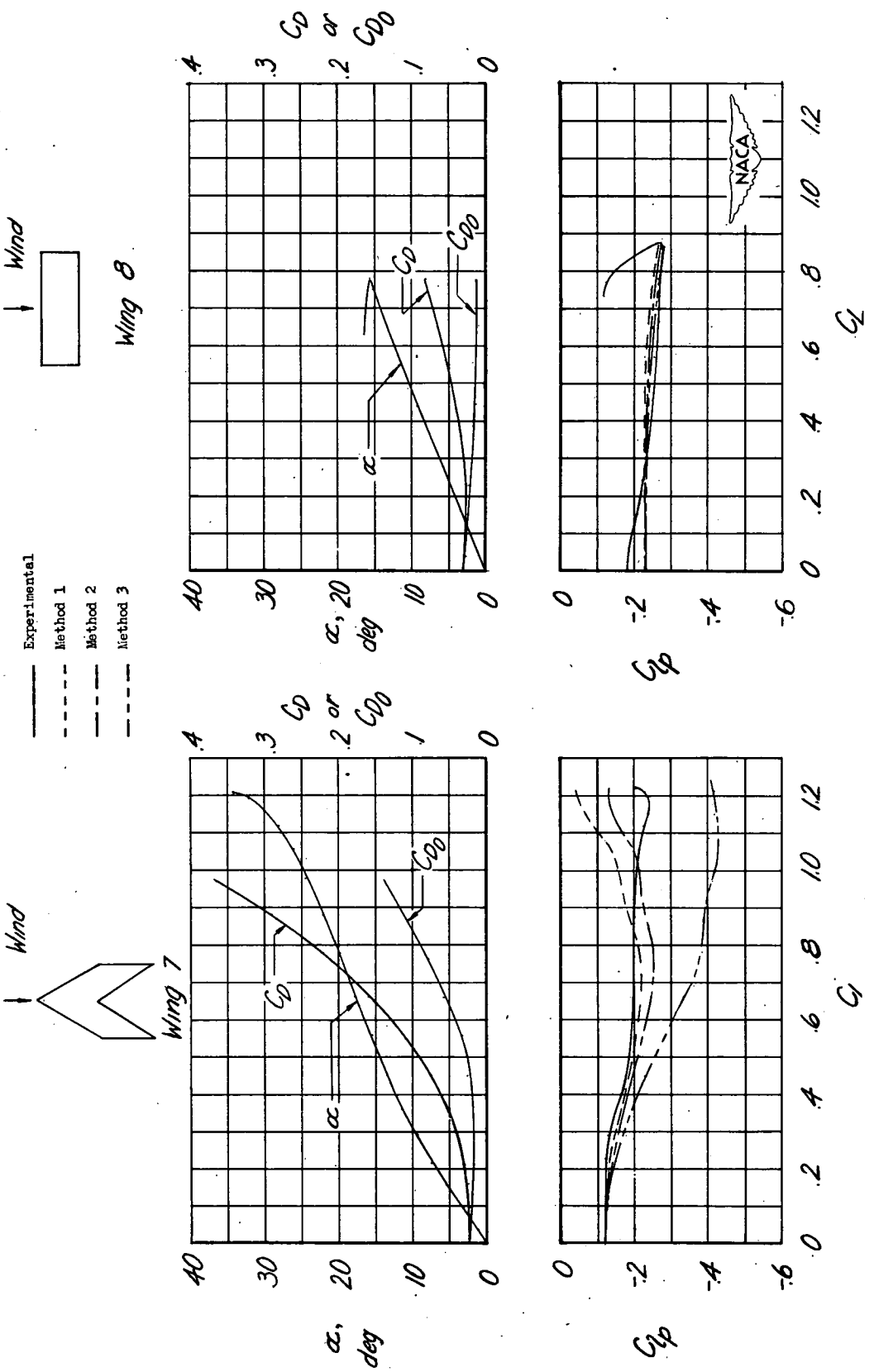

Figure 6.- Estimation of the damping in roll for wings 7 and 8.

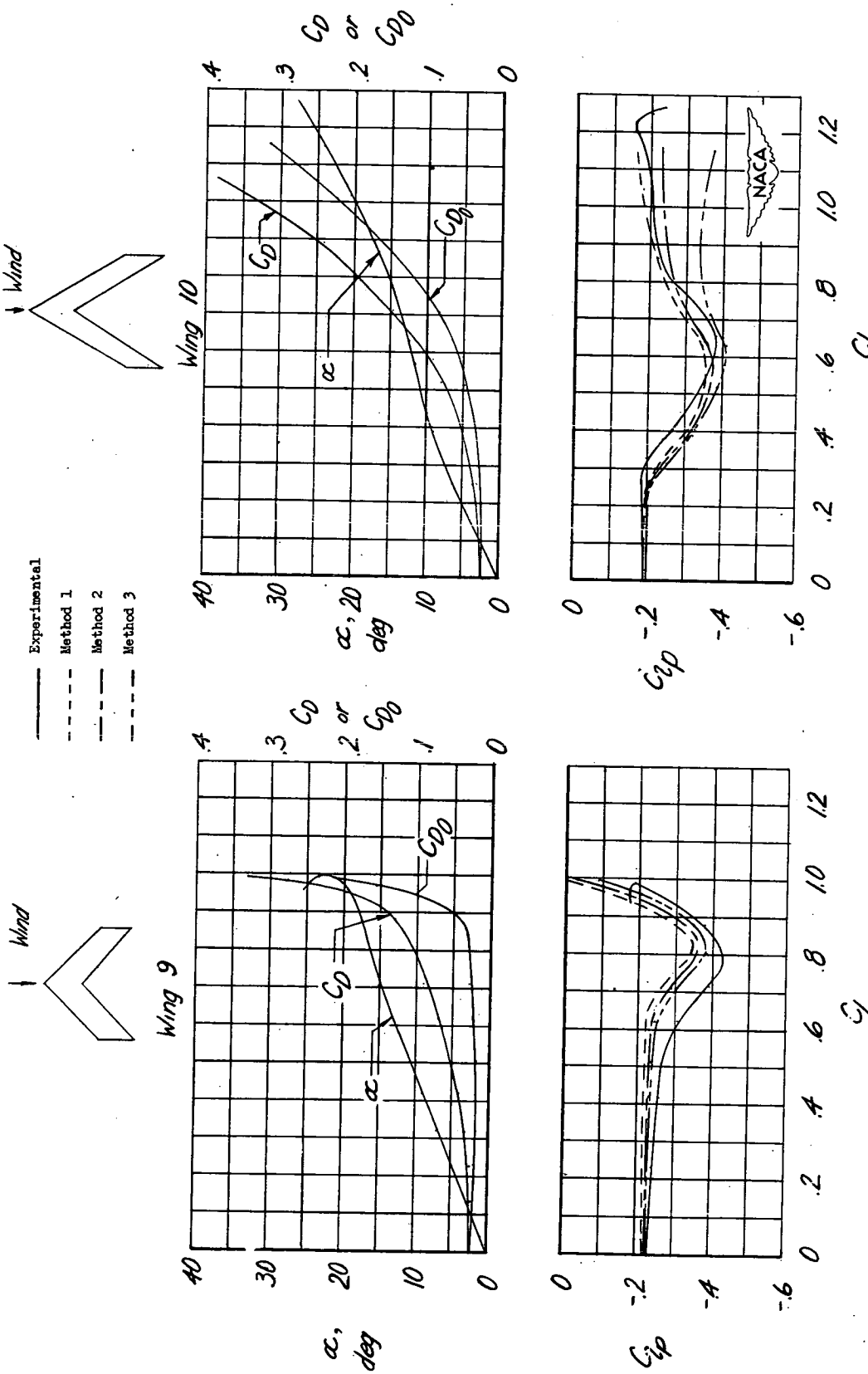

Figure 7.- Estimation of the damping in roll for wings 9 and 10.

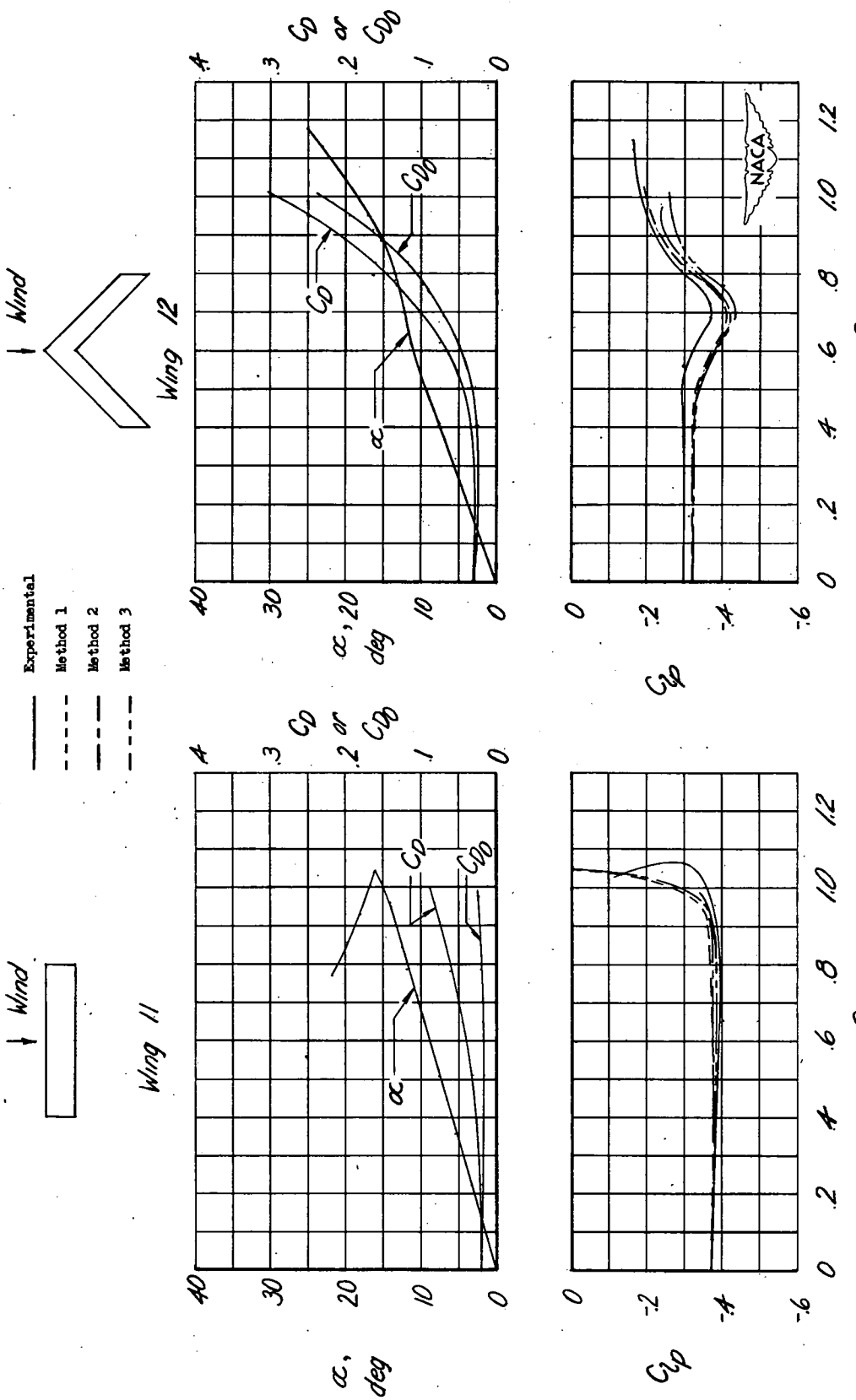

Figure 8.- Estimation of the damping in roll for wings 11 and 12.

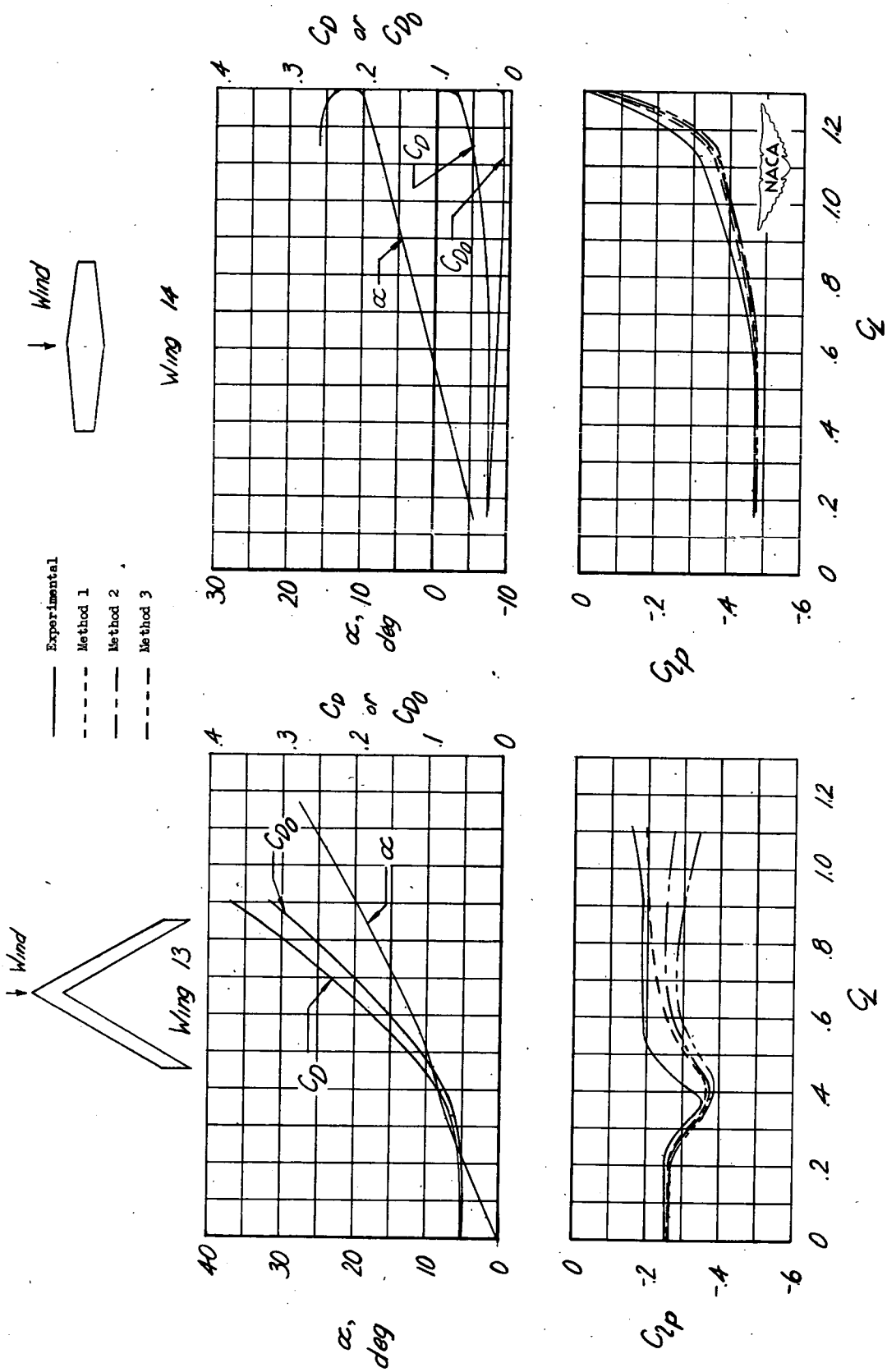

Figure 9.- Estimation of the damping in roll for wings 13 and 14.

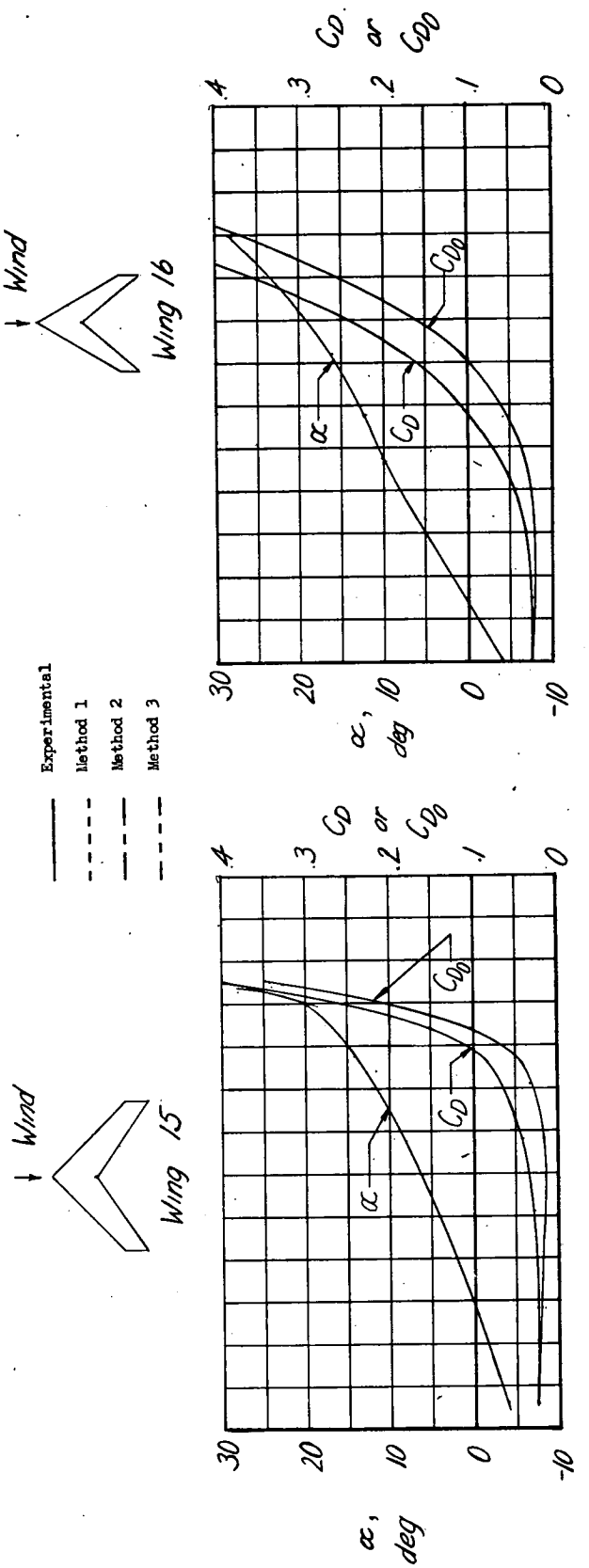

Figure 10.- Estimation of the damping in roll for wings 15 and 16.

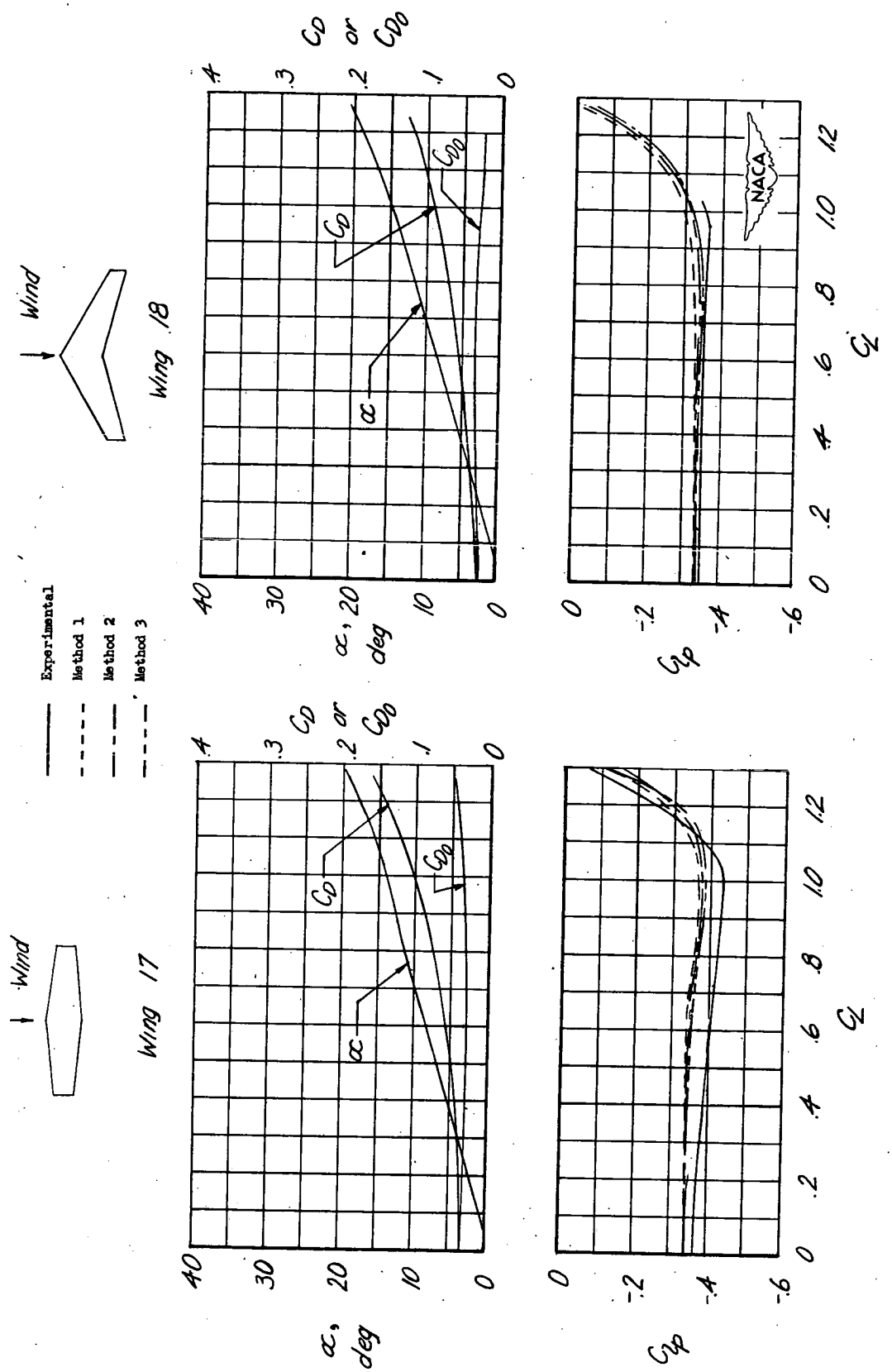

Figure 11.- Estimation of the damping in roll for wings 17 and 18.

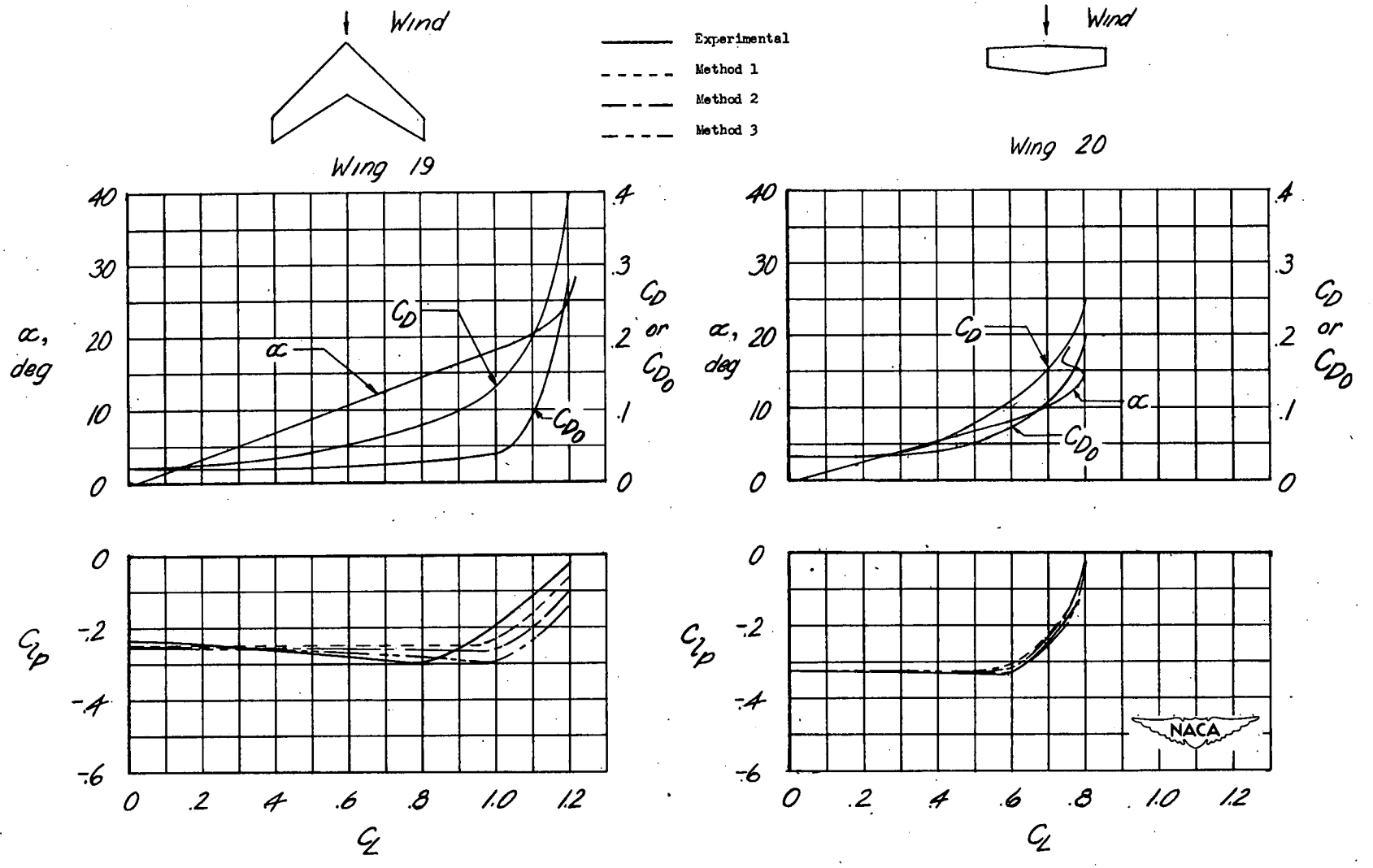

Figure 12.– Estimation of the damping in roll for wings 19 and 20.

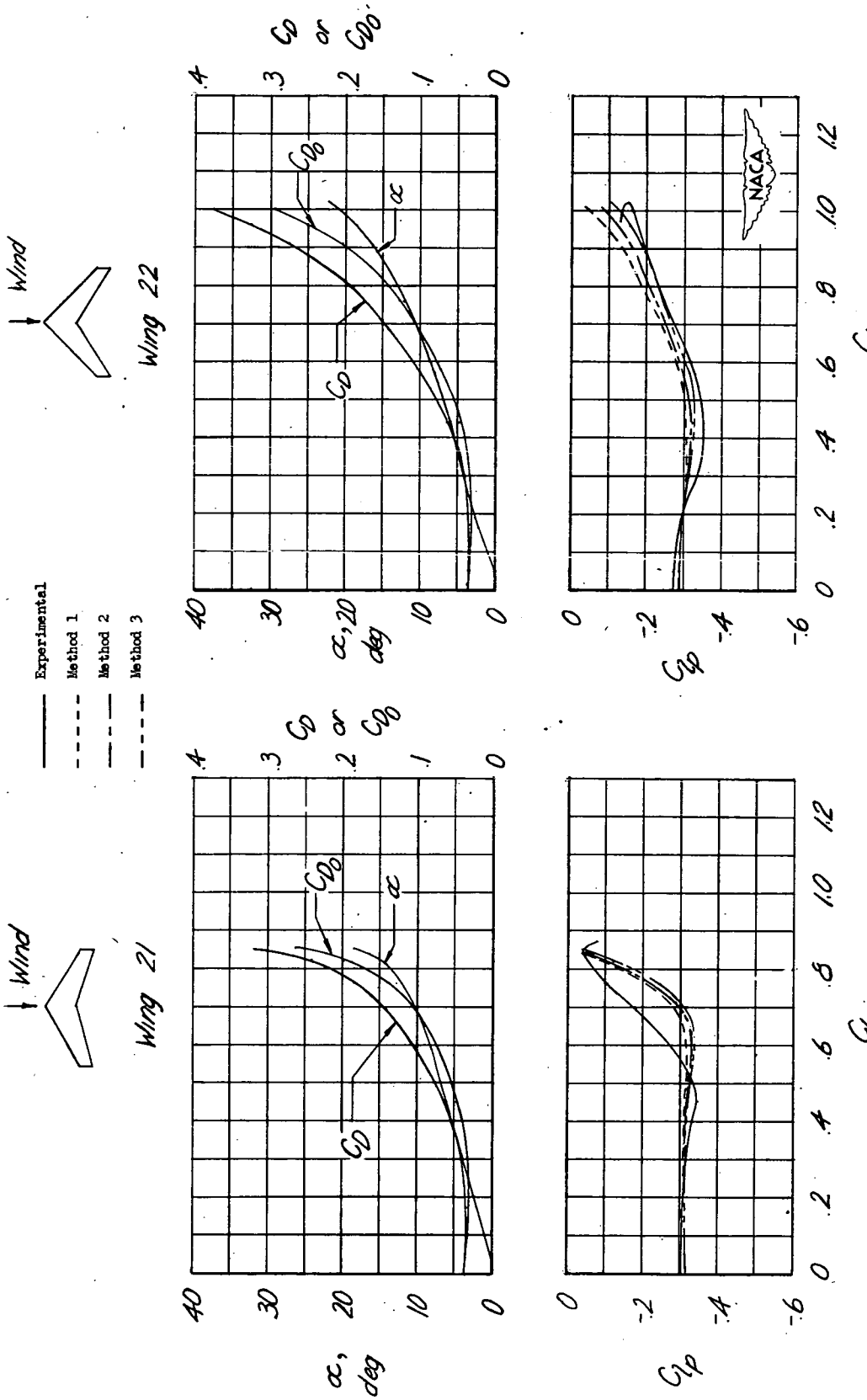

Figure 13.- Estimation of the damping in roll for wings 21 and 22.

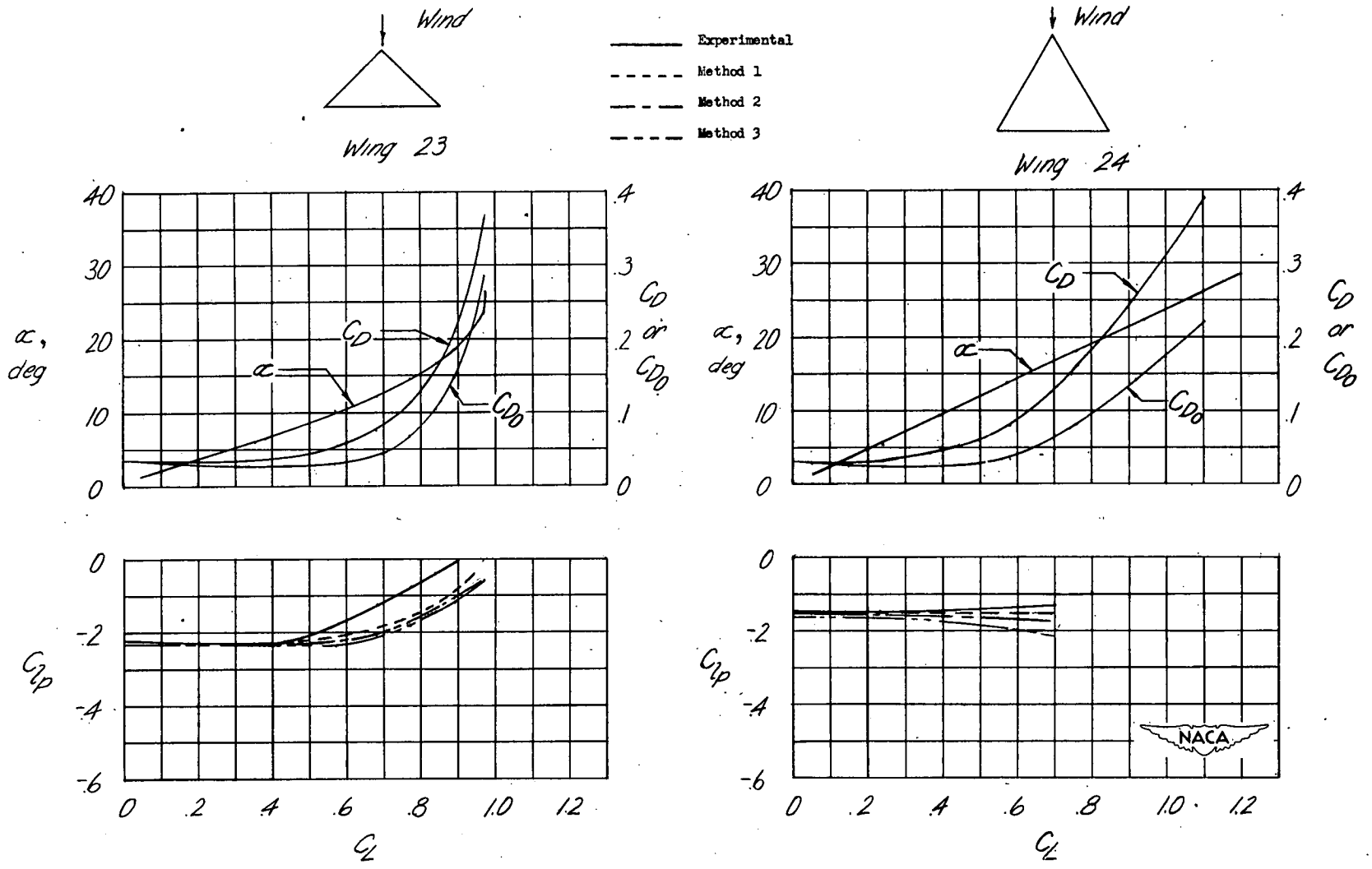

Figure 14.– Estimation of the damping in roll for wings 23 and 24.

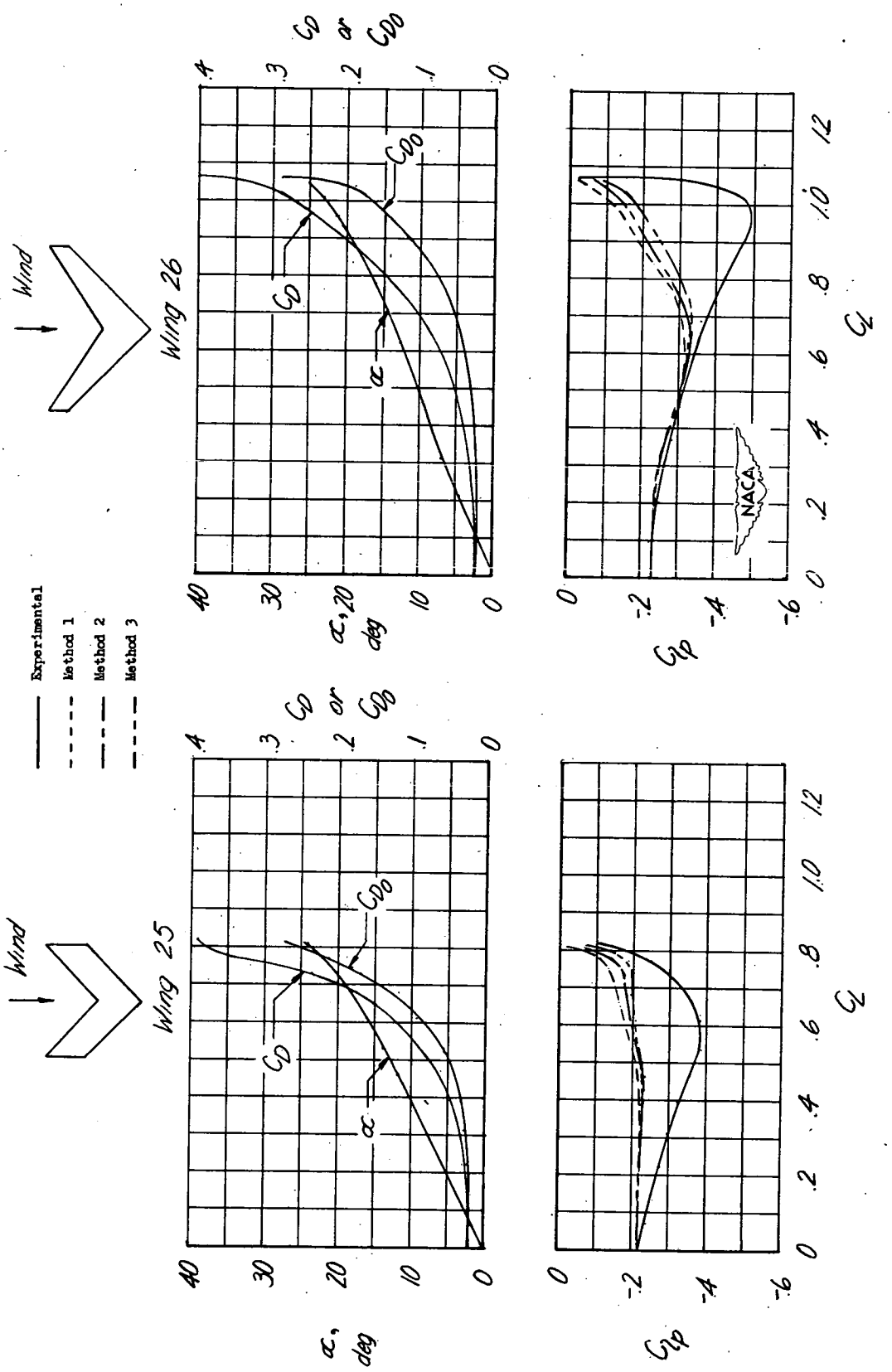

Figure 15.- Estimation of the damping in roll for wings 25 and 26.

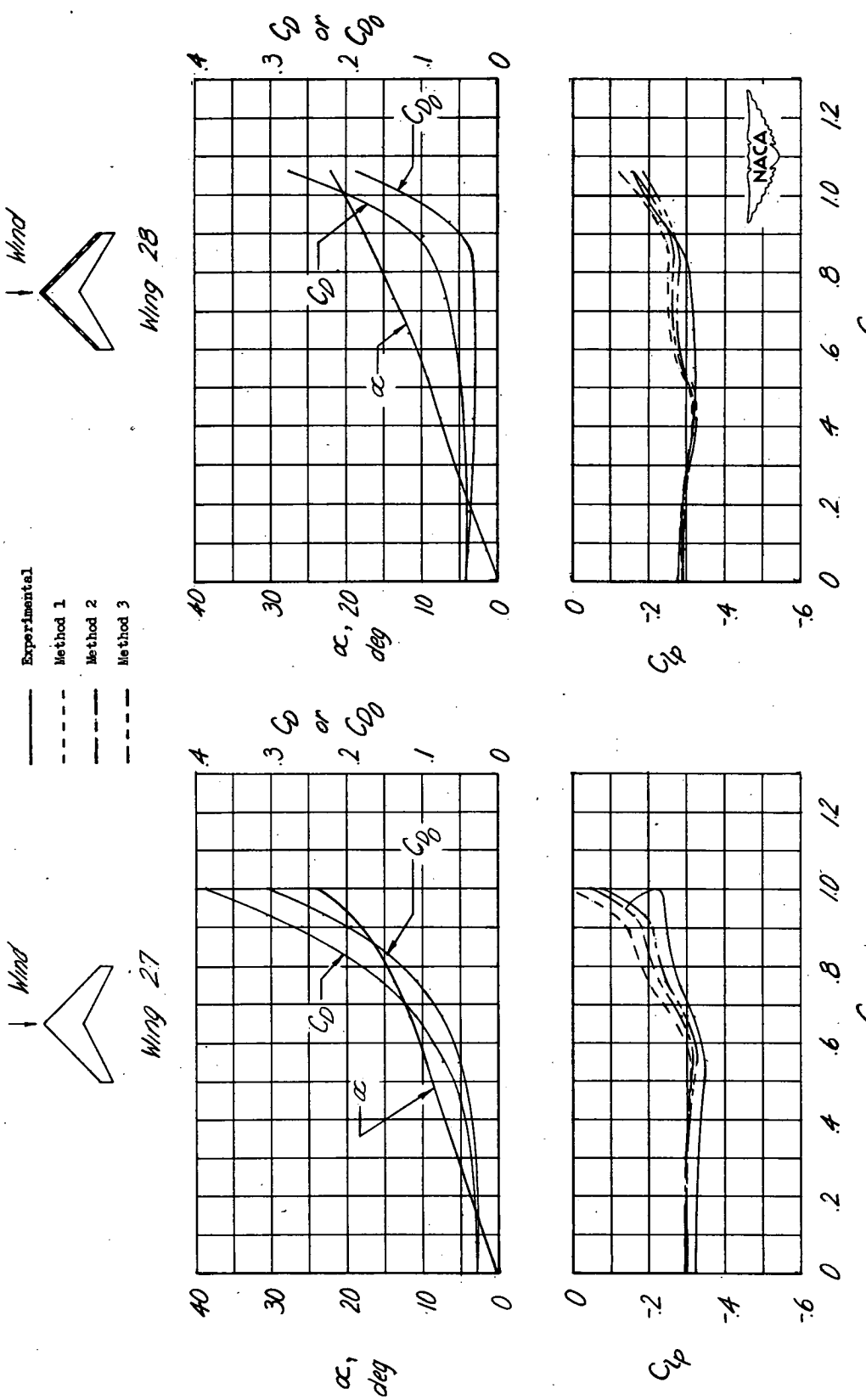

Figure 16.- Estimation of the damping in roll for wings 27 and 28.

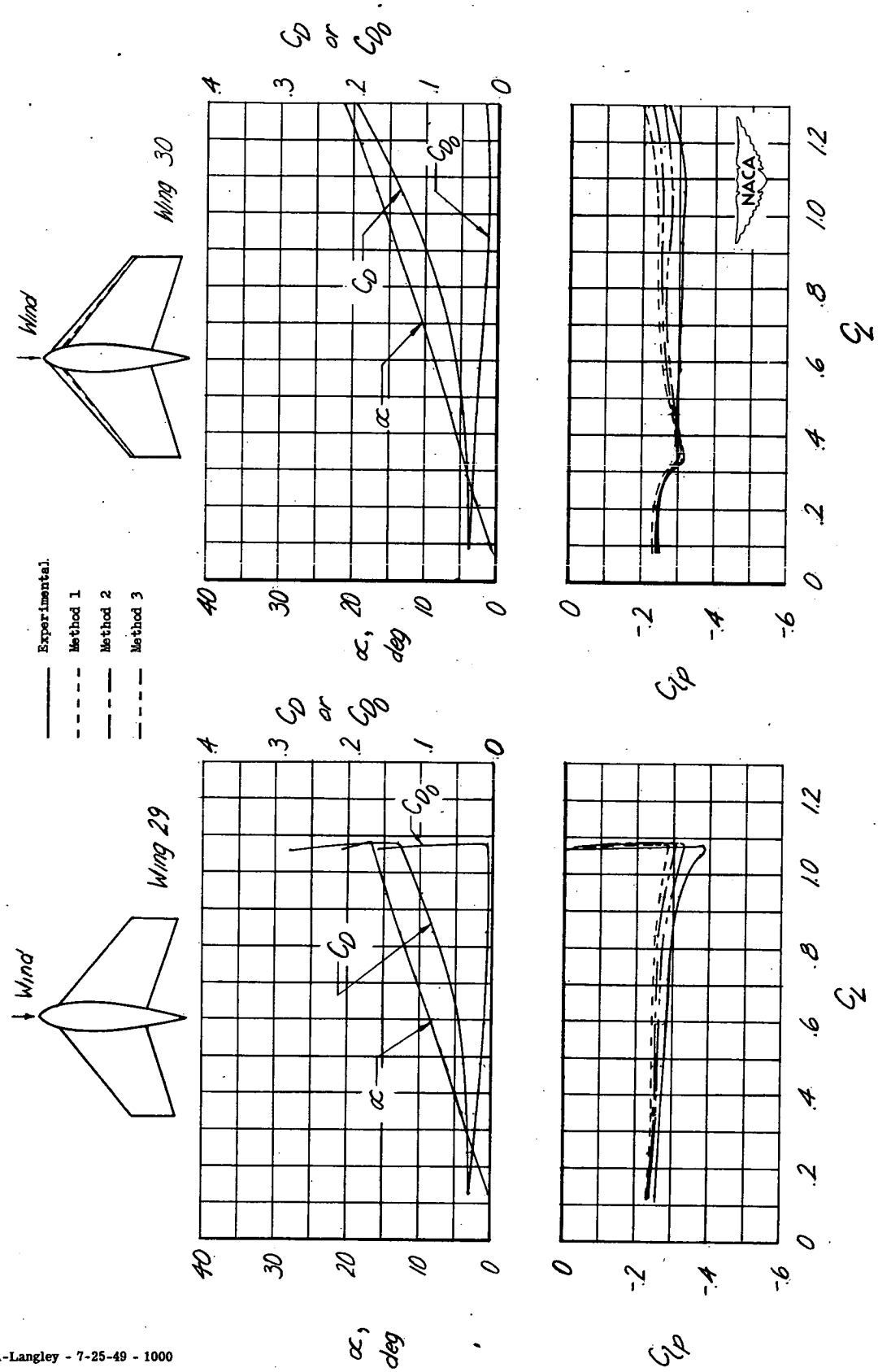

Figure 17.- Estimation of the damping in roll for wings 29 and 30.